Thermodynamics of Protein Hydration Computed by Molecular Dynamics and Normal Modes

Xin Yu, Jongsoon Park,† and David M. Leitner*

Department of Chemistry and Chemical Physics Program, University of Nevada, Reno, Nevada 89557

Received: May 27, 2003; In Final Form: August 27, 2003

Thermodynamic properties of bovine pancreatic trypsin inhibitor (BPTI) hydrated by up to 1600 water molecules, i.e., a ratio of the weight of water to that of protein, h, from 0 to ∼4.5, are studied by molecular dynamics (MD) simulation and normal-mode analysis (NMA). Temperatures range from 100 to 300 K to include the hydrated protein glass transition, $T_g \approx 200$ K. The partial specific heat of BPTI computed by MD reaches fully hydrated values around $h \approx 0.7$ below and above T_g. For smaller h, distinctly different variations in the apparent specific heat of BPTI with h below and above T_g are found and related to the respective decrease and increase in protein flexibility with h. Changes upon varying h in the energy landscape of hydrated BPTI near its native configuration are examined. The partial entropy of BPTI is computed with NMA up to T_g. Above 200 K, an increase in the partial entropy of BPTI is computed with specific heats of hydrated BPTI obtained by MD. The difference between the partial entropy of BPTI when fully hydrated and the entropy of dry BPTI near its native structure is computed to be 0.35 kcal/(mol K). This yields, together with the internal energy difference of −227 kcal/mol, a partial Helmholtz energy of hydrated BPTI that is lower than the Helmholtz energy of dry BPTI by 332 kcal/mol at 300 K. Coverage of BPTI by water correlates with changes in partial thermodynamic properties. A glasslike transition at ∼200 K appears in the computed specific heats when charged groups of BPTI are covered, which occurs when $h \approx 0.3$. Thermodynamic properties reach fully hydrated values when there is little change with increasing h in the coverage of exposed charged and uncharged hydrophilic groups of BPTI, which occurs when $h \approx 0.7$.

1. Introduction

Protein−water interactions mediate protein structure, dynamics, folding, and function, as well as the structure and dynamics of hydration water surrounding the protein.[1−3] One expects, and indeed finds,[4−10] alteration of a protein's thermodynamic properties in the absence or near absence of water. Pioneering measurements of the partial specific heat of hydrated lysozyme by Yang and Rupley provided a systematic analysis of the influence of hydration water on a thermodynamic property of a protein near 300 K.[7] They observed that only a modest number of water molecules per lysozyme, three or four hundred, was sufficient for the partial specific heat to reach its value in the dilute solution limit, and suggested that this corresponds to the amount needed to form one solvation shell around the protein.[7−9] Molecular dynamics (MD) simulations have also provided much insight into the effects of hydration water on protein structure and dynamics.[11−13] Steinbach and Brooks,[11] in their MD study of hydrated myoglobin, again found that hydration by merely a few hundred water molecules is sufficient for the protein's structure and flexibility to converge to those when considerably more water is added. This number of hydration waters was found to correlate with the coverage of charged groups of the protein.[11] MD simulations can also provide information about systematic changes in equilibrium thermodynamic properties of proteins with addition of hydration water, much as MD has been used to elucidate thermodynamic properties of clusters of various sizes.[14−16] In this paper, we report the results of MD simulations and normal-mode analysis (NMA) carried out to explore the effect of hydration water on thermodynamic properties of a protein, and correlate changes in thermodynamic properties with coverage of the protein by hydration water. Computed values of partial heat capacities, entropy, and free energy indicate again that relatively little water is needed for full hydration. We find on the basis of computed specific heats that the onset of a glasslike transition appears near 200 K when charged groups of the protein are covered. Partial thermodynamic properties reach their fully hydrated values when coverage of both charged and uncharged hydrophilic groups no longer changes appreciably upon further hydration.

We address herein the role of hydration water on the partial specific heat, entropy, and free energy of bovine pancreatic trypsin inhibitor (BPTI) as computed by MD and NMA for temperatures ranging from 100 to 300 K. We compute thermodynamic properties over this range of temperature to examine both sides of the hydrated protein glass transition, T_g, which lies near 200 K. While this temperature may or may not correspond to an actual glass transition, a dynamic transition appears in numerous simulations around 200 K,[2,11] and we find in our study a significant drop in the specific heat of hydrated BPTI when the temperature falls below 200 K. Similarly, we find a significant drop in the specific heat of the solvent as the temperature is lowered below about 200 K, and the lowering of the specific heat of hydrated BPTI and that of water below 200 K appear to be coupled. This result is consistent with a large body of work indicating that the protein glass transition is coupled to that of water.[18,19,22−27] We note that the actual

* To whom correspondence should be addressed. E-mail: dml@chem.unr.edu.

† Present address: Department of Physics, Pusan National University, Pusan 609-735, South Korea.

10.1021/jp035471x CCC: $25.00
Published on Web 10/25/2003

glass transition of water has for some time been thought to lie near 135 K,[17] though more recently a higher temperature of around 165 K has been argued,[18,19] the latter corresponding to the protein glass transition in experiments.[20] MD simulations on water reveal a dynamic transition at temperatures not far from 200 K.[21] We shall refer to $T_g \approx 200$ K as the glass transition of the solvent and hydrated protein in our simulations, simply to reflect the sizable differences in the specific heat below and above T_g, though the actual glass transition temperature may be lower. Thermodynamic properties of bulk water are computed to compare with partial properties of hydration water in the fully hydrated limit. This computational study aims to determine how T_g as inferred from the specific heats emerges with hydration, how partial thermodynamic properties vary with hydration below and above T_g, and how such variations correlate with coverage of exposed protein atoms by water molecules. In so doing, we compute differences in the partial specific heat, entropy, and free energy of hydrated and dry BPTI near its native structure.

In the following section we summarize the methods used for computing thermodynamic properties of dry and hydrated BPTI and water by molecular dynamics simulation and normal modes. In section 3 we summarize the thermodynamic quantities that we address in section 4, which presents computational results for the internal energies, heat capacities, entropy, and free energy of hydrated BPTI, and protein coverage by hydration water. Concluding remarks are given in section 5.

2. Computational Methods

In this section we summarize the preparation of the protein−solvent systems, the MD simulations carried out, the energy minimization and NMA for conformations from MD trajectories, and analysis of backbone atom fluctuations obtained by MD and normal modes.

The X-ray crystal structure of BPTI in the Brookhaven Protein Data Bank was used as the starting point for the various simulations. All energy minimization and MD procedures were performed with MOIL,[28] which uses a combination of AMBER, OPLS, and CHARMM force fields. The water molecules in MOIL are represented by the TIP3 potential. Briefly, the initial BPTI structure was minimized and immersed in a box of TIP3 water large enough to accommodate the protein, producing a rectangular solvent box with dimensions of $50 \times 40 \times 56$ Å, containing 3111 water molecules. At this point, another energy minimization was done, followed by MD at 300 K for 10 ps to allow readjustment of the protein and water molecules. Then the solvated protein was used to form different hydration-level structures based on the distance of water molecules to protein atoms. Twenty-three protein−solvent structures at hydration levels of 0, 6, 8, 10, 20, 50, 100, 150, 200, 250, 300, 350, 400, 450, 500, 600, 700, 800, 900, 1000, 1200, 1400, and 1600 waters per protein were obtained. (Dry BPTI, or hydration level 0, corresponds to removal of buried water molecules from the X-ray structure.) Prior to MD, all the different structures were minimized with the conjugate gradient method until the norm of the gradient was less than 0.01 kcal mol^{-1} Å^{-1}. Structures after minimization are referred to as initial structures for further dynamics.

MD simulations were performed on the 23 initial structures at temperatures from 100 to 300 K with 10 K intervals. In all cases, the SHAKE algorithm was employed to constrain all bonds. Velocities were scaled to reach the target temperatures. A total time of 300 ps was covered in the simulations using a 1 fs time step including 100 ps equilibration. A nonbonded atoms list was updated every 0.05 ps, and velocities were scaled every time step. Generated structures and energies were stored in trajectory files every 2 ps, providing 100 conformations and energies for further analysis.

MD simulations on bulk liquid and glassy water were also run to compare with the partial specific heat, entropy, and internal energy of hydration water computed for BPTI in the fully hydrated limit. Bulk glassy water was prepared by simulations beginning with 432 TIP3 water molecules in the ice Ih structure in a box with dimensions $26.34 \times 22.81 \times 21.51$ Å, so that the density is 1.0 g/cm^3. The ice was then heated to 300 K by MD simulation with periodic boundary conditions for 20 ps. Energy minimization with periodic boundary conditions then provided the initial structure for subsequent simulations. Thermodynamic properties of bulk water were obtained with 90 ps MD simulations that included 10 ps equilibration times at temperatures from 100 to 300 K in 10 K intervals. In addition, NMA on a cluster of 735 water molecules was also carried out to obtain the vibrational specific heat and entropy. The cluster was formed after a box was filled with water and all but the closest 735 molecules to the center were removed. The same energy minimization criteria as used for hydrated BPTI, discussed below, were used for the water cluster prior to computation of normal modes.

Energy minima of the hydrated BPTI and bulk water systems were computed by periodic quenching along a trajectory. Hydrated BPTI was quenched every 20 ps over 200 ps constant-temperature simulations for BPTI at hydration levels of 0, 50, 100, 150, 200, 250, 300, 350, 400, 450, 500, 600, 700, 800, 900, 1000, 1200, 1400, and 1600 waters per protein. Simulations were run at temperatures from 200 to 300 K in intervals of 20 K. We thereby obtained 10 conformations that were quenched for every hydration level at each temperature. In some cases, if evaporation happened at some higher temperatures (260 K or higher), average energy minima were obtained for 10 conformations prior to evaporation. All the extracted conformations were subjected to energy minimization with the conjugate gradient method until the norm of the gradient was <0.01 kcal mol^{-1} Å^{-1}. The average energy minimum for the 10 conformations at each temperature was then computed.

Normal modes were computed for 10 conformations each at hydration levels of 0, 100, 200, 300, 400, 500, 600, and 700 waters per protein from MD simulations at 160 and 260 K. Energy minimization was performed for each conformation with the conjugate gradient method until the norm of the gradient was <0.001 kcal mol^{-1} Å^{-1}. The normal-mode frequencies for the 10 conformations at each hydration level were then computed to determine the vibrational specific heat and entropy.

The mass-weighted root-mean-square (RMS) fluctuations of residue positions, averaged over the backbone atoms (N, Cα, C), were computed by MD simulations as

$$\mathrm{RMS}_i = \left\langle \frac{m_{\mathrm{N}}(\mathbf{r}_{\mathrm{N},i} - \bar{\mathbf{r}}_{\mathrm{N},i})^2 + m_{\mathrm{C}\alpha}(\mathbf{r}_{\mathrm{C}\alpha,i} - \bar{\mathbf{r}}_{\mathrm{C}\alpha,i})^2 + m_{\mathrm{C}}(\mathbf{r}_{\mathrm{C},i} - \bar{\mathbf{r}}_{\mathrm{C},i})^2}{m_{\mathrm{N}} + m_{\mathrm{C}\alpha} + m_{\mathrm{C}}} \right\rangle^{1/2} \quad (1)$$

where i labels a residue, m is the mass of the atom, the bar denotes the mean position of the atom over the trajectory, and the angular brackets denote the average over the trajectory. RMS fluctuations were computed over 90 ps at 160 and 260 K following a 10 ps equilibration time starting with the initial structures. RMS fluctuations were also computed for the harmonic BPTI systems using normal modes. In this case,[29] the RMS fluctuations are given by

$$\mathrm{RMS}_i^{\mathrm{nm}} = (kT)^{1/2}\sum_{\gamma}\frac{m_{\mathrm{N}}e_{\mathrm{N},i}{}^{\gamma} + m_{\mathrm{C}_\alpha}e_{\mathrm{C}_\alpha,i}{}^{\gamma} + m_{\mathrm{C}}e_{\mathrm{C},i}{}^{\gamma}}{\omega_\gamma(m_{\mathrm{N}} + m_{\mathrm{C}_\alpha} + m_{\mathrm{C}})} \quad (2)$$

where $e_{\mathrm{N},i}{}^{\gamma}$ is the eigenvector component for backbone atom N of residue i corresponding to mode γ, ω_γ is the frequency of that mode, and k is Boltzmann's constant.

3. Thermodynamic Properties

Here we briefly summarize the thermodynamic properties that we compute by simulation and with normal modes. Our binary system is protein (BPTI) and water. We shall refer to the water as subsystem 1 with thermodynamic property X_1, and the protein as subsystem 2 with thermodynamic property X_2. In what follows, X can be U, C_v, S, and A, namely, the internal energy, specific heat, entropy, and Helmholtz energy, respectively. For this binary system the thermodynamic property X, expressed per unit mass of the mixture, is

$$X = w_1\bar{X}_1 + w_2\bar{X}_2 \quad (3)$$

where $\bar{X}_j$ is the partial property per unit mass of component j with weight fraction w_j. The change in X due to mixing water and protein is

$$\Delta X = X - (w_1X_1^\circ + w_2X_2^\circ) \quad (4)$$

where X_j° is the property per unit mass of pure component j. Let X_ϕ be the apparent property per unit mass of the protein, defined by[30]

$$X_\phi = \frac{X - w_1X_2^\circ}{w_2} \quad (5)$$

The property of mixing per unit mass of the mixture can be expressed in terms of the apparent property of the protein as

$$\Delta X = w_2(X_\phi - X_2^\circ) \quad (6)$$

In the fully hydrated limit $\bar{X}_1 = X_1^\circ$, and we label $\bar{X}_2^\circ = \bar{X}_2$, so that $\bar{X}_2^\circ = X_\phi$. More generally, defining h as the ratio of the weight of water to the weight of protein, $h = w_1/w_2$, we can express the partial properties per unit mass at any h as[30]

$$\bar{X}_1 = X_1^\circ + \frac{\mathrm{d}X_\phi}{\mathrm{d}h} \quad (7a)$$

$$\bar{X}_2 = X_\phi - h\frac{\mathrm{d}X_\phi}{\mathrm{d}h} \quad (7b)$$

A major focus of our computational study of protein hydration aims to find the number of water molecules required to reach the fully hydrated limit, how this correlates with coverage of the protein by the water molecules, and values for the partial properties of the protein and hydration water.

4. Results and Discussion

A. Internal Energy. Figure 1 shows the internal energy per unit mass of hydrated BPTI computed by MD at temperatures of 240 and 300 K, plotted as a function of the weight fraction of protein, w_2. To find the partial energies of BPTI in the dilute solution limit, all points corresponding to BPTI with at least 250 waters, or $w_2 < 0.6$, are fit to a line at each temperature. The fits do not include the internal energies obtained for bulk liquid water (at density 1.0 g/cm^3) at these temperatures, which

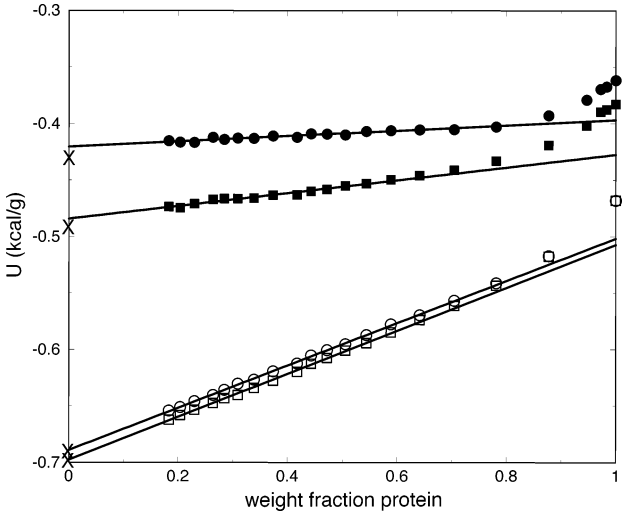

Figure 1. Internal energy per unit mass, U, of dry and hydrated BPTI as a function of the weight fraction of protein, w_2, computed by MD at temperatures of 300 K (filled circles) and 240 K (filled squares). Also plotted is the average energy minimum per unit mass at 300 K (open circles) and 240 K (open squares). Lines are fits through the data at each temperature in the fully hydrated limit, taken to be $w_2 < 0.6$, a range that corresponds to BPTI hydrated by 250−1600 water molecules. Internal energies and average energy minima computed for bulk water at these temperatures are all indicated by "X".

we find to be −0.4337 and −0.4952 kcal/g at 300 and 240 K, respectively. The extrapolated partial energies of water in the fully hydrated limit, $U_1^\circ = -0.4206$ and −0.4844 kcal/g at 300 and 240 K, respectively, come reasonably close to the bulk values. At 300 K, all energies for BPTI with at least 100 water molecules lie near the line, while at 240 K at least 200 or 250 water molecules are required for the partial internal energy of hydrated BPTI to reach its value in the fully hydrated limit. The intercept of these lines at $w_2 = 1$, the pure protein, gives the partial internal energy per unit mass of BPTI in the fully hydrated limit, $\bar{U}_2^\circ$. We find $\bar{U}_2^\circ = -0.3970$ kcal/g and $\bar{U}_2^\circ = -0.4277$ kcal/g at temperatures of 300 and 240 K, respectively. Since the internal energy of the pure protein is computed to be $U_2^\circ = -0.3618$ and −0.3829 kcal/g at 300 and 240 K, respectively, the internal energy of mixing in the dilute solution limit is $\Delta U = -0.0352$ kcal/g of BPTI at 300 K and −0.0448 kcal/g of BPTI at 240 K, which corresponds to −227 kcal/mol in the former case and −289 kcal/mol in the latter.

Lowering of the partial internal energy of BPTI with hydration corresponds to lowering of the configurational energies due to protein−solvent interactions, so it is of interest to compute energy minima at these temperatures. A protein can be found in one of many conformational substates at 240 and 300 K,[31,32] the potential energies of which can be found by quenching structures obtained in the MD simulation.[31,33] Average energy minima of hydrated BPTI as a function of the weight fraction of protein, w_2, are plotted in Figure 1. The energies that are plotted are averages over 10 quenched structures from the simulation. We again fit all data for $w_2 < 0.6$ to obtain partial energy minima for BPTI in the fully hydrated limit. Extrapolating to $w_2 = 1$, we find in the fully hydrated limit $\bar{U}_2^\circ = -0.5020$ and −0.5076 kcal/g at 300 and 240 K, respectively. The average energy minima computed for the pure protein are identical at these two temperatures, $U_2^\circ = -0.4673$ kcal/g. We thereby obtain an average energy minimum of mixing of −224 kcal/mol at 300 K, essentially the same as −227 kcal/mol found above by plotting the total energies of hydrated BPTI. At 240 K, we find the energy of mixing using the quenched energies

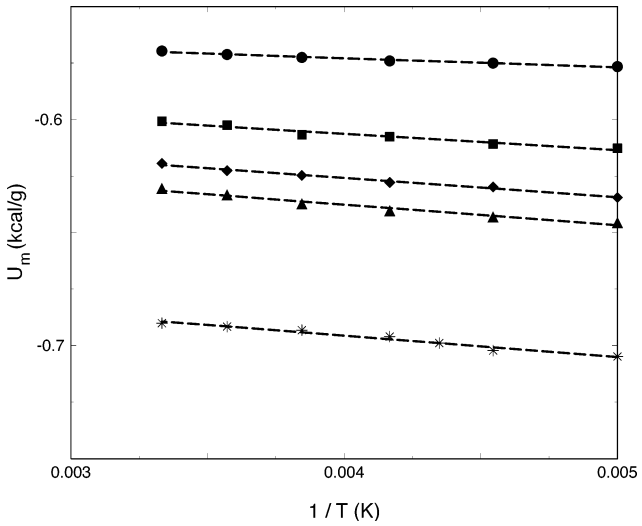

Figure 2. Energy minima, U_m, averaged over 10 quenched structures from MD simulation as a function of $1/T$ for temperatures from 100 to 300 K. Results for BPTI with 200 (circles), 400 (squares), 600 (tilted squares), and 800 (triangles) water molecules and bulk water (asterisks) are plotted. Dashed lines are linear fits through the data.

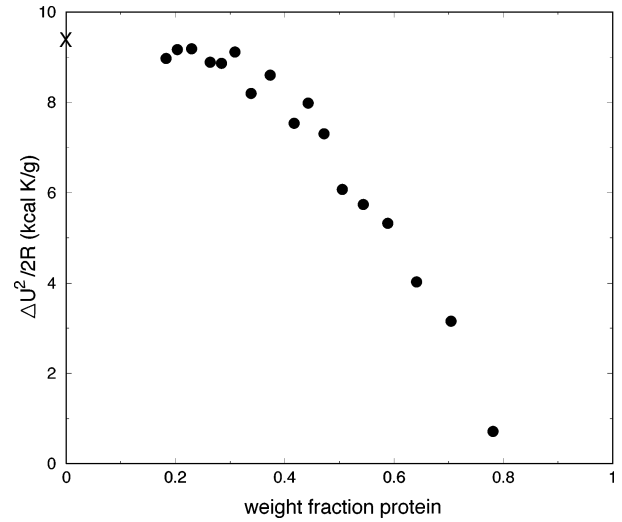

Figure 3. $\Delta U^2/2R$ for hydrated BPTI as a function of the weight fraction of protein, w_2, obtained from the slope of U_m vs $1/T$. The result computed for bulk water is also plotted (X). Values for hydrated protein appear to approach that for water when $w_2 < 0.3$.

to be −260 kcal/mol, comparable to the value of −289 kcal/mol found with the total energies, though not as close as what we find at 300 K.

We now explore properties of the energy landscape of hydrated BPTI near its native structure. From the energy landscape theory of proteins,[34,35] the average energy minimum for a protein around a given structure (a given stratum of the protein folding funnel) varies according to the random energy model as

$$U_m(T) = \bar{U} - \frac{\Delta U^2}{2RT} \tag{8}$$

where $\bar{U}$ is the mean energy of the landscape at this stratum (here near the native structure), ΔU is the "ruggedness", and R is the gas constant. Energies of inherent structures of glass-forming liquids have been argued to follow the same form,[36,37] which has been demonstrated for water above 200 K in simulations.[38,39] Plotting U_m against $1/T$ should thus give a straight line at low temperatures whose slope provides information about the ruggedness of the energy landscape.

We plot U_m (kcal/g) against $1/T$ for several hydrated BPTI systems and for bulk water in Figure 2. In each case we observe that the points fall on a straight line for temperatures from 200 to 300 K. The absolute values of the slopes of the lines fit to the plots of U_m against $1/T$ are plotted in Figure 3. We observe that as water is added the data appear to approach a value of 9.0 (kcal K)/g, close to the value we find from our simulations on bulk water of 9.3 (kcal K)/g. It appears, then, that the contribution of ruggedness to the average energy minimum increases as water is added until the value for the solvent is reached, in this case with addition of 800 water molecules. Since this value does not appear to vary with further addition of water, we estimate the partial ruggedness of the BPTI energy landscape in the hydrated limit, $\Delta\bar{U}_2°$, is about 16 kcal/mol. Using this value, we find, for example, that in the hydrated limit $-(\Delta\bar{U}_2°)^2/2RT$ is −215 and −268 kcal/mol at 300 and 240 K, respectively. These values are close to the difference between the partial energy of hydrated BPTI and internal energy of dry BPTI at these temperatures, suggesting that the differences arise in large part from the ruggedness of the energy landscape of BPTI near its native structure that appears with addition of water.

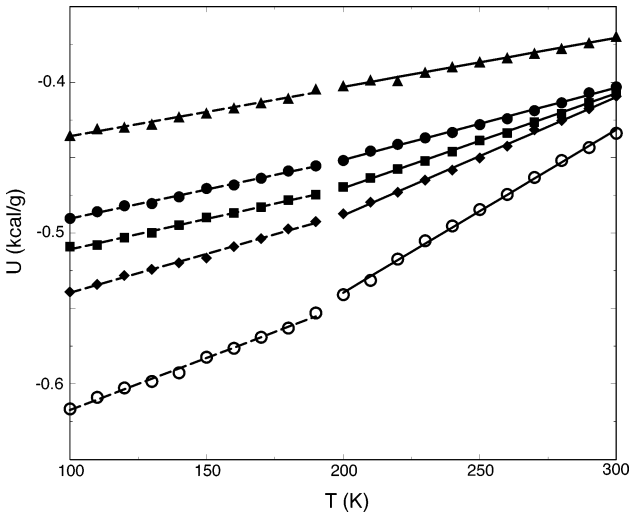

Figure 4. Internal energy per unit mass, U, computed by MD as a function of temperature for BPTI hydrated by 10 (triangles), 100 (filled circles), 200 (squares), and 400 (tilted squares) water molecules. Also plotted is U computed for bulk water (open circles). Linear fits through the data below and above 200 K are indicated to illustrate the difference in specific heats of hydrated BPTI below and above this temperature.

B. Heat Capacity. Figure 4 shows the average internal energy per unit mass computed at temperatures from 100 to 300 K for BPTI with 10, 100, 200, and 400 water molecules, as well as simulated bulk liquid water for comparison. We group results for the internal energies below and above 200 K and analyze them separately. The slopes of lines fit through the data give us specific heats. A fit through the data below $T_g \approx 200$ K generally yields a distinctly smaller specific heat than that obtained by fitting through the data from temperatures of 200 K and higher. For BPTI with only 10 water molecules, the specific heat below and above T_g is nearly the same. As more waters are added for the systems shown, the specific heat above T_g becomes ever greater than that below it. The slopes below and above T_g approach those fit to the results for bulk water as the protein becomes more hydrated.

In the analysis that follows, we obtain the specific heat below T_g by taking the slope of a fit to the internal energies computed from 100 to 180 K in intervals of 10 K. We use the internal energies computed from 220 to 300 K in intervals of 10 K to

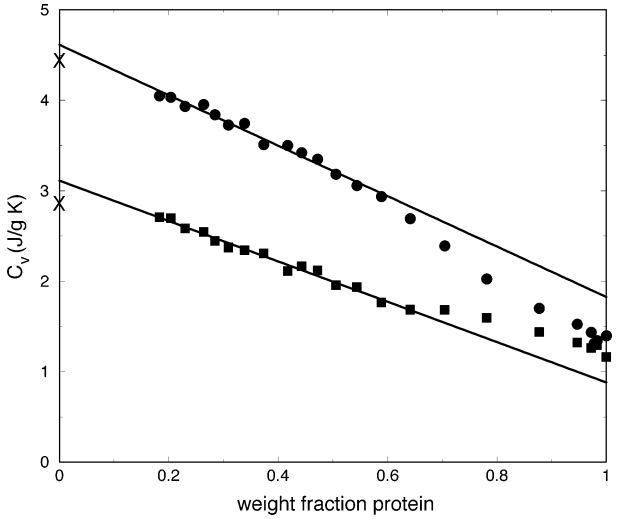

Figure 5. Specific heat, C_v, for dry and hydrated BPTI and bulk water (X) below (squares) and above (circles) T_g, computed by MD, as a function of the weight fraction of protein, w_2. Lines are fits through the data in the fully hydrated limit, $w_2 < 0.6$. Extrapolation to $w_2 = 1$ gives the partial specific heat of BPTI in the fully hydrated limit of 0.88 J/(g K) below and 1.83 J/(g K) above T_g.

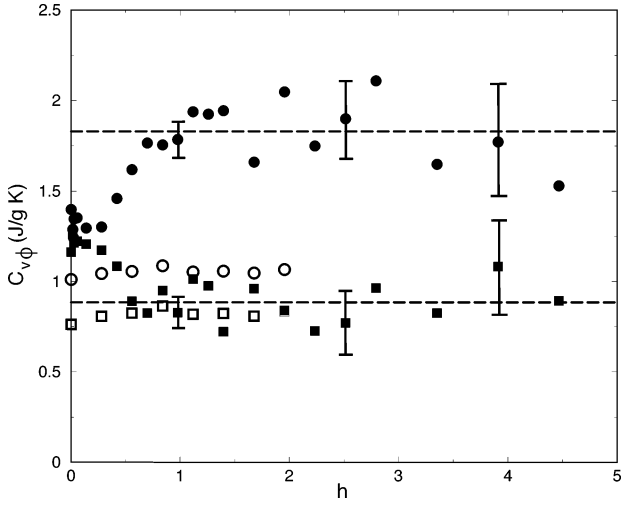

Figure 6. Apparent specific heat, $C_{v\phi}$, of BPTI below (filled squares) and above (filled circles) T_g computed by MD as a function of h, the ratio of the weight of water to the weight of protein. Also plotted is the apparent specific heat of BPTI at 200 K (open squares) and 300 K (open circles) computed with normal modes. Dashed lines are the partial specific heats for BPTI below and above T_g, found by extrapolation of the full hydration limit fits in Figure 5 to $w_2 = 1$. Error bars, estimated from the fits in Figure 5, are indicated for some of the data.

determine the specific heat above T_g. These sets of results for different levels of hydration are plotted in Figure 5. Results for the specific heat of bulk liquid and glassy water are included for comparison, but are not used for fitting data in the fully hydrated limit.

When the protein is dry or nearly dry, the specific heats obtained below and above T_g are found to be similar. For dry BPTI they are found to be 1.2 and 1.4 J/(g K), respectively, and for BPTI with six water molecules they are both around 1.3 J/(g K). As more water molecules surround BPTI, particularly beyond 100 or so, the specific heats below and above T_g begin to diverge and ultimately fall around two distinct lines. Specific heats below and above 200 K are fit for all BPTI hydrated with at least 250 water molecules, $w_2 < 0.6$, up to the largest number of 1600 used in the simulations. The specific heats computed for pure glassy and liquid water at a density of 1.0 g/cm^3 are plotted for comparison but are not used for the fits; extrapolation to $w_2 = 0$ comes reasonably close to the computed pure water results. We note that both extrapolated results of the fits to the fully hydrated protein data and the similar specific heats computed for bulk glassy and liquid water are all rather high. We find the partial specific heat of the hydration water in the fully hydrated limit, $C^\circ_{v,1}$, to be 4.6 J/(g K) and the specific heat for bulk water to be 4.4 J/(g K) when it should be 4.2 J/(g K) at 300 K.[40] We find $C^\circ_{v,1}$ for the glassy hydration water to be 3.1 J/(g K) in the fully hydrated limit and C_v for glassy bulk water to be 2.8 J/(g K), whereas the actual value is closer to 2 J/(g K) around 200 K.[40] Indeed, we obtain 1.6 J/(g K) for pure water at 200 K with normal-mode analysis. Values computed by MD are high because vibrational contributions are overestimated, particularly at lower temperatures. Extrapolation of the line fit through the data in the fully hydrated limit, when BPTI is hydrated by at least 250 water molecules, to $w_2 = 1$, the pure protein, gives the partial specific heat of the protein in the fully hydrated limit, $\bar{C}^\circ_{v,2}$. Below the glass transition we find $\bar{C}^\circ_{v,2} = 0.88$ J/(g K), whereas above it we find $\bar{C}^\circ_{v,2} = 1.83$ J/(g K).

Yang and Rupley[7] analyze the apparent specific heat, $C_{v\phi}$, which they measure for hydrated lysozyme near 300 K. To compare at least qualitatively with results of their analysis, we compute the apparent specific heat of BPTI, $C_{v\phi}$, with eq 5 using the value of $\bar{C}^\circ_{v,1}$ in the fully hydrated limit given above both below and above T_g. The results are plotted in Figure 6. The figure suggests essentially three regions in h both below and above the glass transition where the apparent specific heat varies in a distinct way, variations defining regions similar to those found in ref 7.[41] We shall discuss each of these three regions in turn.

Above T_g, the fully hydrated limit is observed to lie above $h \approx 0.7$ ($\sim$250 water molecules), whereas the limit appears to lie above $h \approx 0.55$ ($\sim$200 water molecules) below T_g. In this fully hydrated region, the first of the three regions mentioned above, the apparent specific heat of the protein appears to fluctuate around $\bar{C}^\circ_{v,2} = 0.88$ J/(g K) below T_g and $\bar{C}^\circ_{v,2} = 1.83$ J/(g K) above T_g, as expected. Results tend to fluctuate increasingly around the limiting values as h increases, a result of increasing numerical uncertainty with larger h. Error bars given for some of the data in the figure indicate this trend.

Monotonic approach to the fully hydrated limit both below and above T_g appears to begin with roughly 100 water molecules, or $h \approx 0.28$. The approach to the fully hydrated limit can be identified as a second region in the apparent specific heats computed for BPTI. The value of $C_{v\phi}$ rises to the fully hydrated limit above T_g, whereas it decreases to the fully hydrated limit below T_g. Equations 7a and 7b can be used to find the partial specific heats in this region. Below T_g, we find $\bar{C}_{v,1} = 2.22$ J/(g K) and $\bar{C}_{v,2} = 1.43$ J/(g K); above T_g we find $\bar{C}_{v,1} = 5.72$ J/(g K) and $\bar{C}_{v,2} = 0.99$ J/(g K). In this region, the partial specific heat of the protein below T_g is roughly what it is for the pure protein above T_g, whereas the partial specific heat of the protein above T_g is very roughly what it is for the pure protein below T_g. The rise in the apparent specific heat above T_g in this region is due to the increasing availability of higher energy configurations with temperature as we increase the number of water molecules, as revealed in the energy landscape analysis above. The lowering of the apparent specific heat of BPTI with increasing number of water molecules from 100 to 200 below T_g is most likely due to increasing rigidity of the protein as water is added (vide infra). Apparent specific heats at 200 K obtained from normal modes, also plotted in Figure 7, indicate that the specific heat for the purely harmonic

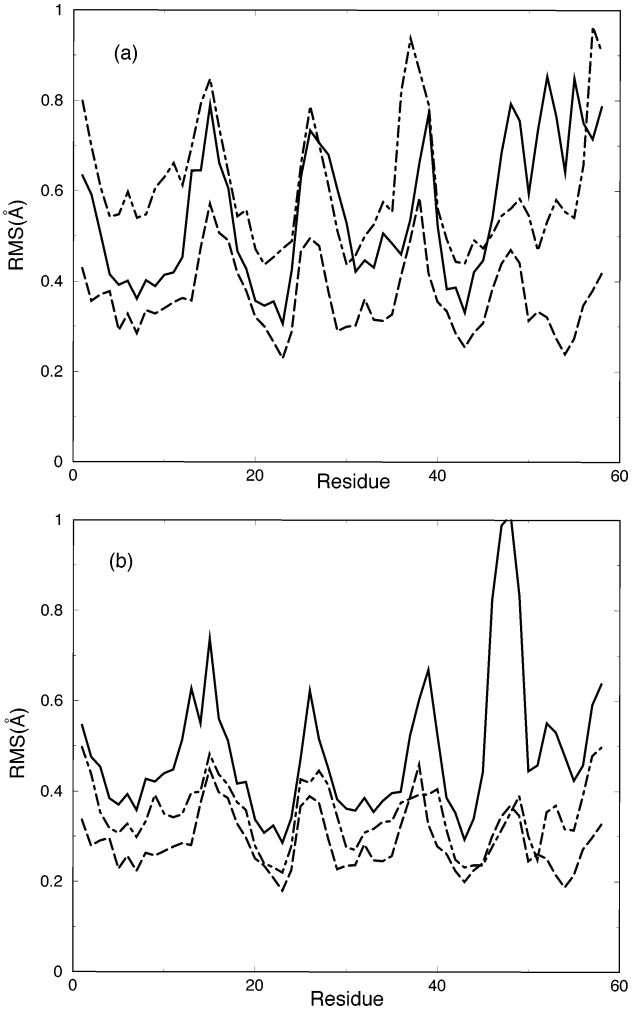

Figure 7. Mass-weighted root-mean-square fluctuations of protein backbone atoms at temperatures of (a) 260 K and (b) 160 K. Plotted are results from 90 ps simulations for dry BPTI (solid curve) and BPTI with 200 water molecules (dotted−dashed curve) and from normal modes for dry BPTI (dashed curve).

vibrations does not decrease below T_g in this region of h. The specific heat of hydrated BPTI is computed by summing over all normal modes, α, with frequency ω_α:

$$C_{v,\mathrm{nm}} = \sum_\alpha k\left(\frac{\hbar\omega_\alpha}{kT}\right)^2 \frac{e^{-\hbar\omega_\alpha/kT}}{(1-e^{-\hbar\omega_\alpha/kT})^2} \qquad (9)$$

where k is Boltzmann's constant and $\hbar$ is Planck's constant over 2π. The results from MD simulations below T_g appear to come quite close to the purely harmonic results computed with normal modes at 200 K when h, the ratio of the weight of water to the weight of protein, is at least 0.5.

The third identifiable region in the variation of the apparent specific heat with h is the limit of very little water ($h < 0.2$). Here, though there is some fluctuation in the data, $C_{v\phi}$ seems to decrease some with increasing h above T_g and to increase some or remain nearly constant with increasing h below T_g. Using $C_{v\phi}$ computed for BPTI with no water molecules, and with 6, 8, 10, and 20 water molecules, we can estimate the partial specific heat of water in this region with eq 7. We find, both above and below T_g, that the specific heat of water in this regime lies around 4 J/(g K), between the partial values for glassy and liquid water in the fully hydrated limit of 3.1 and 4.6 J/(g K), respectively. We note, however, that not enough data in this region are available for a more reliable estimate for the partial specific heat of water when there are so few water molecules present.

The diverging values of $C_{v\phi}$ below and above T_g in the second region, $h \approx 0.3-0.7$, suggest very different dynamical trends with hydration. Indeed, Steinbach and Brooks[11] point out in a simulation study of myoglobin that increasing hydration increases protein flexibilites at temperatures above T_g, whereas it decreases protein flexibility at temperatures below T_g. To see if we find similar trends for BPTI, we compute the RMS fluctuations of backbone atoms of BPTI, using both the full dynamics, eq 1, and normal modes, eq 2. Results for the mass-weighted RMS fluctuations averaged over backbone atoms (N, C_α, C) of each residue are plotted in Figure 7. RMS fluctuations were computed by MD over a 90 ps interval at (a) 260 K and (b) 160 K, for dry BPTI and BPTI with 200 water molecules; also shown are the RMS fluctuations computed with normal modes. For the latter, the results plotted are averages computed for 10 structures of dry BPTI quenched over the same 90 ps interval; we note that we found RMS fluctuations computed with normal modes for all structures along the MD simulation to be very similar.

At 260 K, above T_g, we observe that the RMS fluctuations of BPTI with 200 water molecules are usually largest, followed by those of dry BPTI, and finally those of harmonic BPTI computed by NMA. On average, RMS fluctuations per residue are 0.55 Å for dry BPTI, 0.60 Å for BPTI with 200 water molecules, and 0.36 Å for harmonic BPTI. An increase in RMS fluctuations with increasing hydration is consistent with the changes in the energy landscape discussed above. At low levels of hydration, one might expect significant contributions of anharmonic vibrations to protein motions and the specific heat, i.e., oscillations whose amplitudes increase with temperature around the same minimum in the potential. With more water molecules, anharmonic vibrations around one minimum or perhaps several close in energy might give way to transitions to higher lying minima and ultimately a wider range of motions of the protein, and a larger configurational contribution to the specific heat. We see in Figure 7a that RMS fluctuations for residues 46−58 of dry BPTI are larger than for the hydrated protein, reflecting the sizable structural adjustment of this portion of the protein away from the initial structure of the dry protein over this time period. For the other residues, 1−45, RMS fluctuations of the hydrated protein are greater than for the dry one by about 0.1 Å per residue on average. Differences between the motion of dry BPTI computed by MD and NMA are also apparent. Although the overall variation of the RMS fluctuations with residue is generally similar for residues 1−45, the amplitude is larger by about 0.15 Å per residue for dry BPTI computed by MD.

Turning to a temperature below T_g, 160 K shown in Figure 7b, we observe a trend different from that found above T_g. In this case, RMS fluctuations of the anharmonic motion of dry BPTI computed by MD are again greater than those of harmonic BPTI computed by NMA, consistent with results of earlier MD and NMA studies of dry BPTI below T_g.[42] When we add 200 water molecules to BPTI, the RMS fluctuations of this system come quite close to those for harmonic BPTI, differing significantly only near the ends of the protein. Overall, average RMS fluctuations are 0.35 and 0.48 Å per residue for BPTI with and without water, respectively, and 0.29 Å for dry BPTI computed by NMA. As suggested by the specific heat data, hydrated BPTI is noticeably harmonic below the glass transition, in contrast to what is typically found above it.

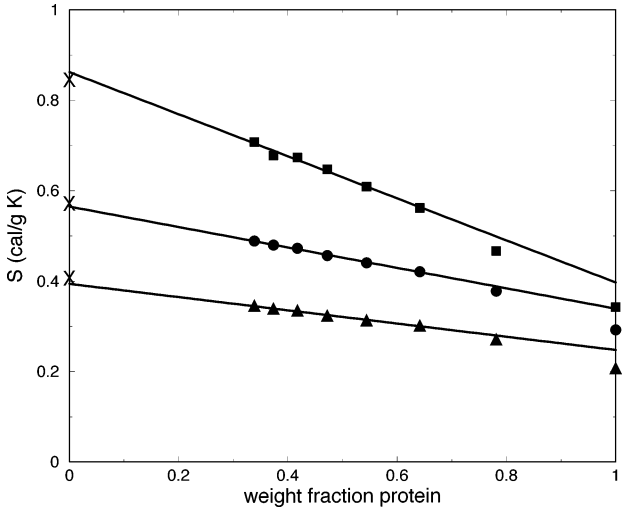

Figure 8. Entropy, S, of dry BPTI and BPTI hydrated by up to 700 water molecules as a function of the weight fraction of BPTI, w_2. The entropy computed with normal modes, S_{nm}, is plotted at 300 K (circles) and 200 K (triangles), while the entropy computed by normal modes up to 200 K and MD at higher temperatures is plotted at 300 K (squares). (See eq 11.) The partial entropy of BPTI and water in the full hydration limit is found at each temperature by fitting S and S_{nm} where $w_2 < 0.7$. Extrapolation to the $w_2 = 1$ intercept gives for the partial vibrational entropy of BPTI values of 1.60 and 2.19 kcal/(mol K) at 200 and 300 K, respectively, and for the partial entropy at 300 K a value of 2.56 kcal/(mol K). Extrapolation to $w_2 = 0$ gives 7.1 and 10.2 cal/(mol K) for the vibrational entropy of water at 200 and 300 K, respectively, and 15.5 cal/(mol K) for the entropy of water at 300 K. Similar values are found for bulk water (X), which were not used for fitting the data. The difference between the partial entropy of fully hydrated BPTI and the entropy of dry BPTI at 300 K is 0.35 kcal/(mol K), while the corresponding difference in the vibrational entropy at 300 K is 0.30 kcal/(mol K).

C. Entropy. The entropy of hydrated BPTI above T_g can be estimated using the computed heat capacities if we have reference values for the entropy. To obtain the reference values, we shall assume that below the glass transition the entropy can be computed from the normal modes of both dry and hydrated BPTI. The entropy computed with normal modes, S_{nm}, is given by the sum of contributions from each mode α as

$$S_{nm} = \sum_{\alpha} \frac{\hbar\omega_\alpha/T}{e^{\hbar\omega_\alpha/kT} - 1} - k \ln(1 - e^{-\hbar\omega_\alpha/kT}) \qquad (10)$$

We compute S_{nm} for dry BPTI and BPTI with up to 700 water molecules in intervals of 100. The average value of S_{nm} for each system is computed with the normal modes of 10 structures obtained from a 200 ps MD simulation at 260 K. Results for S_{nm} at temperatures of 200 and 300 K are plotted in Figure 8 as a function of the weight fraction of protein, w_2. Fits to the vibrational entropy, S_{nm}, in the fully hydrated limit, i.e., hydration with at least 200 water molecules ($w_2 < 0.7$), are plotted to obtain the partial entropy of BPTI and water in the limit of full hydration. Extrapolation to pure water, $w_2 = 0$, gives the partial harmonic vibrational entropy of hydration water, $S^\circ_{nm,1}$, in the fully hydrated limit at 200 and 300 K. We obtain values of 7.1 cal/(mol K) at 200 K and 10.2 cal/(mol K) at 300 K. The former is close to the entropy of glassy water that we compute with the normal modes of water, which turns out to be the same as the actual entropy of ice at 200 K, 7.4 cal/(mol K).[40] The latter is close to the entropy of water again computed with the normal modes of water, 10.4 cal/(mol K), and comparable to the entropy of ice of 9.9 cal/(mol K) at the melting point.[40] Extrapolation to $w_2 = 1$ gives the partial entropy for BPTI computed with normal modes in the fully hydrated limit. We find the partial vibrational entropy of BPTI to be higher than the vibrational entropy of dry BPTI by 0.26 and 0.30 kcal/(mol K) at 200 and 300 K, respectively.

Assuming $S = S_{nm}$ up to 200 K for BPTI at all levels of hydration, we compute the increase in entropy above T_g using the specific heats computed by MD. The entropy of hydrated BPTI at 300 K is then given by

$$S(300\text{ K}) = S_{nm}(200\text{ K}) + C_v \ln\left(\frac{3}{2}\right) \qquad (11)$$

Our results for S(300 K) are also plotted in Figure 8. Fitting the entropy of BPTI hydrated with at least 200 water molecules allows us to estimate the partial entropy of water and BPTI in the fully hydrated limit. Extrapolation to $w_2 = 0$ gives 15.5 cal/(mol K) for the entropy of water at 300 K. This value is close to the entropy we obtain for pure water computed again with eq 11, using normal modes up to 200 K and the specific heat computed by MD above T_g. The computed pure water entropy is 15.2 cal/(mol K) at 300 K, which can be compared with the actual value of 16.5 cal/(mol K).[40] Our approach depends, of course, on the value we use for T_g. If T_g is 190 K rather than 200 K, as is very plausible judging from Figure 5, we obtain 16.0 cal/(mol K) for the entropy of water. Extrapolation of the fully hydrated BPTI results to $w_2 = 1$ gives 2.56 kcal/(mol K) for the partial entropy of BPTI in the fully hydrated limit, or 0.35 kcal/(mol K) greater than the entropy of pure BPTI. The entropy of hydrating BPTI, $\Delta S \approx 0.35$ kcal/(mol K), is about 0.05 kcal/(mol K) greater than what we found with the normal modes alone.

Our result for the difference between the partial entropy of BPTI when fully hydrated and the entropy of dry BPTI, 0.35 kcal/(mol K), together with the corresponding internal energy difference of -227 kcal/mol, yields at 300 K a partial Helmholtz energy of BPTI that is lower than the Helmholtz energy of dry BPTI by 332 kcal/mol. The actual number of water molecules need only be about 250 or so to attain this free energy difference.

D. Hydration. In this section we examine the coverage of exposed atoms of BPTI by water molecules as the protein becomes hydrated. Specifically, we look at 10 structures of each of the hydrated BPTI systems with up to 700 water molecules over a 200 ps trajectory at 260 K to find those atoms of BPTI that come within 3.5 Å of an atom of any water molecule. We classify only heavy atoms of BPTI as exposed. These include non-hydrogen atoms that fall within 3.5 Å of a water molecule, as well as the heavy atoms attached to hydrogens of BPTI that lie within 3.5 Å of a water molecule. In all, we find 251 exposed atoms out of a total of 448 heavy atoms in BPTI. We have classified the exposed atoms as charged, uncharged hydrophilic, or hydrophobic, as in ref 11. The 32 charged atoms include those on the N and C termini as well as atoms on the end groups of Asp, Glu, Arg, and Lys. The 110 uncharged hydrophilic atoms include all other O and N atoms, as well as C and S atoms with charge greater than 0.31e. The remaining 109 exposed carbon atoms are classified as hydrophobic.

We have determined the fraction of each of these categories of exposed BPTI atoms that are in fact covered by a water molecule at any one time for BPTI with 10, 20, 50, and 100−700 water molecules in intervals of 100. The results are plotted in Figure 9. For charged atoms we observe a rapid rise in coverage as hydration water is added until about 100 waters

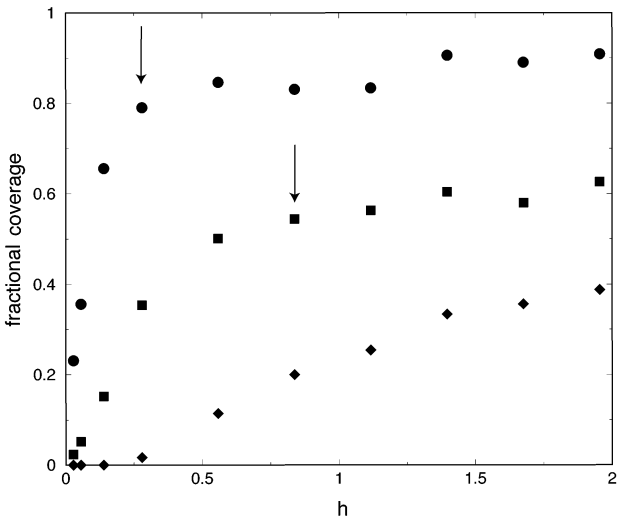

Figure 9. Average fractional coverage of exposed heavy atoms of BPTI by water molecules at any one time as a function of *h*, the ratio of the weight of water to the weight of protein. Exposed atoms are those atoms of BPTI for which a water molecule was found to be within 3.5 Å during simulations of BPTI hydrated by up to 700 water molecules. If this atom of BPTI is a hydrogen atom, then the attached heavy atom is classified as exposed. Fractional coverage that is plotted is an average over 10 structures at each level of hydration at which the fraction of exposed atoms covered by water was computed. Exposed atoms are classified as charged (circles), uncharged hydrophilic (squares), and hydrophobic (tilted squares). For the former two, a region of rapid rise of coverage with hydration can be roughly separated from a region where the coverage changes relatively little with hydration. An arrow indicates approximate crossover between these regions.

are present, at which point about 80% of the 32 exposed charged atoms are covered by at least one water molecule at any one time. Addition of hydration water beyond 100 only slowly changes the fractional coverage, which approaches about 0.9 with 700 waters. Uncharged hydrophilic atoms of BPTI are increasingly covered by water molecules up to roughly 200−300 water molecules ($h \approx 0.7$), at which point about 60% of these exposed atoms are covered by at least one water molecule at any one time. Additional hydration does not change much the fractional coverage of uncharged hydrophilic groups. The fraction of exposed hydrophobic atoms does not appear to reach or approach any limit over the range of systems examined, but instead rises steadily as the number of hydration waters increases to 700, reaching a fractional coverage of about 0.4 at any one time with this many water molecules.

It appears, then, that as exposed charged and uncharged hydrophilic groups of the protein begin to saturate, so too do thermodynamic properties. While roughly half of the exposed uncharged hydrophilic groups are still unoccupied at any given time when BPTI is surrounded by 200−300 water molecules, this fraction does not change much as more water is added, in contrast to the sharp rise with *h* when there are fewer water molecules. This correlates quite well with the values of *h* where the apparent specific heats of BPTI reach their fully hydrated values, both below and above the glass transition. The full hydration limit appears to be determined by the number of charged groups and uncharged hydrophilic groups on the surface of the protein, and the value of *h* at which the full hydration limit is reached would be therefore protein-dependent. Not surprisingly, *h* to reach this limit is higher for a small protein such as BPTI, with a relatively large surface-to-volume ratio, than it is for larger proteins such as lysozyme and myoglobin.

5. Concluding Remarks

We have computed changes in thermodynamic properties of BPTI with the addition of hydration water by molecular dynamics simulations and by computation of normal modes. Partial internal energies, heat capacities, and entropy for BPTI near its native structure were computed over a sizable range in the number of hydration waters and at temperatures below and above a glasslike transition temperature, T_g. The specific heats computed for the solvent and hydrated protein indicate that $T_g \approx 200$ K. The appearance of T_g with hydration of BPTI correlates with coverage of charged groups of the protein. Partial thermodynamic properties of BPTI reach their full hydration limit values when the average fractional coverage of both charged groups and exposed uncharged hydrophilic groups at any one time does not change much with further hydration.

The average internal energies of hydrated BPTI were computed by MD simulation for temperatures ranging from 100 to 300 K. For dehydrated BPTI and BPTI with low levels of hydration essentially only one value of the specific heat was apparent from the data for this temperature range. With sufficient hydration to cover charged groups of BPTI, about 100 water molecules, two distinct values of the specific heat, one below and one above $T_g \approx 200$ K, become apparent, approaching with increasing hydration the values computed for bulk water below and above $T_g \approx 200$ K. When there is little rise in coverage of charged and exposed uncharged hydrophilic groups of the protein as more water is added, the partial specific heat of BPTI reaches its value in the fully hydrated limit. The partial specific heat of BPTI is larger for the fully hydrated protein than for the dry protein at temperatures above T_g, and is smaller for the fully hydrated protein than the dry protein below T_g. The partial specific heat of the protein increases with hydration above T_g due to the accessibility, upon interaction with water, of higher lying minima in the potential as the temperature is increased. The hydrated protein is generally more flexible than the dry protein at temperatures above the glass transition temperature and less flexible at temperatures below T_g,[11,12] as revealed, for example, by RMS fluctuations of backbone atoms.

The entropy of hydrated BPTI and of water below T_g was computed with normal modes. An increase in entropy above T_g was computed using specific heats obtained by MD, where we used $T_g = 200$ K. Computed values for the partial entropy of hydration water in the full hydration limit and of bulk water were similar to each other, and both close to the actual entropy of water. The difference between the partial entropy of fully hydrated BPTI and that of dry BPTI was computed to be 0.35 kcal/(mol K). The corresponding difference in the internal energy at 300 K was computed to be −227 kcal/mol, yielding a difference in the partial Helmholtz energy of fully hydrated BPTI and dry BPTI of about −330 kcal/mol at 300 K.

Some trends in thermodynamic properties of hydrated BPTI that we have found are consistent with other studies of hydration. Computation of the entropy of BPTI with and without a buried water molecule using normal modes indicates a rise in the entropy of the protein upon interaction with water.[6,43] Molecular dynamics simulations examining the structure and flexibility of myoglobin with a wide range of hydration waters at 300 K reveal both the greater stability and greater flexibility with hydration.[11] A relatively small number of water molecules, around 350 and corresponding to the number needed to cover charged groups, was found to be sufficient to reach the fully hydrated limit as determined by protein structure and flexibility. Yang and Rupley[7] inferred from their calorimetric measurements

of hydrated lysozyme crystals that fewer than 400 water molecules are required for the partial specific heat of lysozyme to reach the limit of a dilute aqueous solution, an amount that they suggested would allow for uniform coverage of the protein. This work suggests something in between. Establishing $T_g \approx$ 200 K requires coverage of charged groups of the protein, in agreement with the conclusion of ref 11. However, partial thermodynamic properties converge to their full hydration limit values when coverage of both charged groups and uncharged hydrophilic groups at any one time remains essentially constant upon further hydration. For BPTI, coverage of charged groups and establishment of $T_g \approx 200$ K occur with hydration by about 100 water molecules, while more than twice this many are needed for complete hydration.

We have examined here the role of hydration water on equilibrium thermodynamic properties of a protein. Beyond equilibrium properties, one would like to understand the role of water in nonequilibrium properties, too, such as thermal transport. Energy flow in a molecule mediates rates of chemical reactions.[44] Thermal energy is carried by protein vibrations, which are coupled to vibrations of water. The coefficient of thermal conductivity is also proportional to the heat capacity. Assuming that merely vibrations contribute to the heat capacity, and that the vibrations can be approximated by normal modes and low-order anharmonic corrections, we have computed the coefficient of thermal conductivity for myoglobin to be 2.0 W cm^{-1} K^{-1} at 300 K, about one-third the value for water.[45] Computation of the partial specific heat of hydrated BPTI by MD in this study suggests that the coefficient of thermal conductivity may well be 50% or so larger than that computed with normal modes.

Acknowledgment. This work was supported by the National Science Foundation (Grant NSF CHE-0112631), a New Faculty Award from the Camille and Henry Dreyfus Foundation, and a Research Innovation Award from the Research Corp.

References and Notes

(1) Gregory, R. B., Ed. *Protein−Solvent Interactions*; Marcel Dekker: New York, 1995.
(2) Bizzarri, A. R.; Cannistraro, S. *J. Phys. Chem. B* **2002**, *106*, 6617.
(3) Merzel, F.; Smith, J. C. *Proc. Natl. Acad. Sci. U.S.A.* **2002**, *99*, 5378.
(4) Kunz, I. D.; Kauzmann, W. *Adv. Protein Chem.* **1973**, *28*, 239.
(5) Rupley, J. A.; Careri, G. *Adv. Protein Chem.* **1991**, *41*, 37.
(6) Fischer, S.; Smith, J. C.; Verma, C. S. *J. Phys. Chem. B* **2001**, *105*, 8050.
(7) Yang, P. H.; Rupley, J. A. *Biochemistry* **1979**, *18*, 2654.
(8) Finney, J. L.; Poole, P. L. *Comments Mol. Cell. Biophys.* **1984**, *2*, 129.
(9) Gregory, R. B. *Protein−Solvent Interactions*; Marcel Dekker: New York, 1995; p 191.
(10) Angell, C. A. *Science* **1995**, *267*, 1924.
(11) Steinbach, P. J.; Brooks, B. R. *Proc. Natl. Acad. Sci. U.S.A.* **1993**, *90*, 9135.
(12) Steinbach, P. J.; Brooks, B. R. *Proc. Natl. Acad. Sci. U.S.A.* **1996**, *93*, 55.
(13) Arcangeli, C.; Bizzarri, A. R.; Cannistraro, S. *Chem. Phys. Lett.* **1998**, *291*, 7.
(14) Berry, R. S.; Beck, T. L.; Davis, H. L.; Jellinek, J. *Adv. Chem. Phys.* **1988**, *70*, 75.
(15) Wales, D. J. *Science* **1996**, *271*, 925.
(16) Wales, D. J.; Doye, J. P. K.; Miller, M. A.; Mortenson, P. N.; Walsh, T. R. *Adv. Chem. Phys.* **2000**, *115*, 1.
(17) Mishima, O.; Stanley, H. E. *Nature* **1998**, *396*, 329.
(18) Velikov, V.; Borick, S.; Angell, C. A. *Science* **2001**, *294*, 2335.
(19) Angell, C. A. *Chem. Rev.* **2002**, *102*, 2627.
(20) Green, J. L.; Fan, J.; Angell, C. A. *J. Phys. Chem.* **1994**, *98*, 13780.
(21) Tanaka, H. *Nature* **1996**, *380*, 328.
(22) Iben, I. E. T.; Braunstein, D.; Doster, W.; Frauenfelder, H.; Hong, M. K.; Johnson, J. B.; Luck, S.; Ormos, P.; Schulte, A.; Steinbach, P. J.; Xie, A. H.; Young, R. D. *Phys. Rev. Lett.* **1989**, *62*, 1916.
(23) Tarek, M.; Tobias, D. J. *Phys. Rev. Lett.* **2002**, *88*, 138101.
(24) Vitkup, D.; Ringe, D.; Petsko, G. A.; Karplus, M. *Nat. Struct. Biol.* **2000**, *7*, 34.
(25) Réat, V.; Dunn, R.; Ferrand, M.; Finney, J. L.; Daniel, R. M.; Smith, J. C. *Proc. Natl. Acad. Sci. U.S.A.* **2000**, *97*, 9961.
(26) Fitter, J. *Biophys. J.* **1999**, *76*, 1034.
(27) Doster, W.; Bachleitner, A.; Dunau, R.; Hiebl, M.; Lüscher, E. *Biophys. J.* **1986**, *50*, 213.
(28) Elber, R.; et al. *Comput. Phys. Commun*. **1995**, *91*, 159. The version used for this study was obtained from http://www.tc.cornell.edu/reports/NIH/resource/CompBiologyTools/moil.
(29) Levitt, M.; Sander, C.; Stern, P. S. *J. Mol. Biol.* **1985,** *181*, 423.
(30) See, e.g., Guggenheim, E. A. *Thermodynamics*; North-Holland: Amsterdam, 1967.
(31) Elber, R.; Karplus, M. *Science* **1987**, *235*, 318.
(32) Frauenfelder, H.; Sligar, S. G.; Wolynes, P. G. *Science* **1991**, *254*, 1598.
(33) Stillinger, F. H.; Weber, T. A. *J. Phys. Chem.* **1983**, *87*, 2833.
(34) Bryngelson, J. D.; Wolynes, P. G. *Proc. Natl. Acad. Sci. U.S.A.* **1987**, *84*, 7524.
(35) Onuchic, J. N.; Luthey-Schulten, Z.; Wolynes, P. G. *Annu. Rev. Phys. Chem.* **1997**, *48*, 545.
(36) Speedy, R. J. *J. Phys. Chem. B* **1999**, *103*, 4060.
(37) Heuer, A.; Büchner, S. *J. Phys.: Condens. Matter* **2000**, *12*, 6535.
(38) Sastry, S. *Nature* **2001**, *409*, 164.
(39) Starr, F. W.; Sastry, S.; La Nave, E.; Scala, A.; Stanley, H. E.; Sciortino, F. *Phys. Rev. E* **2000**, *64*, 041201.
(40) Dorsey, N. E. *Properties of Ordinary Water Substance*; Reinhold Publ. Corp.: New York, 1940.
(41) Yang and Rupley also discuss in ref 7 a fourth region, between our first and second regions, in which there appears a slight decrease in $C_{v\phi}$ with increasing h as the full hydration limit is approached. We cannot rule out the possibility of such a region from our data, which could be masked by computational errors in $C_{v\phi}$.
(42) Hayward, J. A.; Smith, J. C. *Biophys. J.* **2002**, *82*, 1216.
(43) Fischer, S.; Verma, C. S. *Proc. Natl. Acad. Sci. U.S.A.* **1999**, *96*, 9613.
(44) Leitner, D. M.; Levine, B.; Quenneville, J.; Martinez, T. J.; Wolynes, P. G. *J. Phys. Chem. A*, in press.
(45) Yu, X.; Leitner, D. M. *J. Phys. Chem. B* **2003**, *107*, 1698.